Formation Acquisition Sensor for the Terrestrial Planet Finder (TPF) Mission

Jeffrey Y. Tien
M/S 138-212
818-393-1642
Jeffrey.Y.Tien@JPL.NASA.gov

Jeffrey M. Srinivasan
M/S 238-212
818-393-6126
Jeffrey.M.Srinivasan@JPL.NASA.gov

Larry E. Young
M/S 138-212
818-354-5018
Lawrence.E.Young@JPL.NASA.gov

George H. Purcell, Jr.
M/S 238-600
818-354-3395
George.Purcell@JPL.NASA.gov

all at
Jet Propulsion Laboratory,
California Institute of Technology
4800 Oak Grove Dr.
Pasadena, CA 91109-8099

Abstract— The Terrestrial Planet Finder (TPF) pre-project, an element of NASA's Origins Program, is currently investigating multiple implementation architectures for finding earth-like planets around other stars. One of the technologies being developed is the Formation Flying Interferometer (FFI). The FFI is envisioned to consist of up to seven spacecraft, each with an infrared telescope, flying in precise formation within ±1 cm of pre-determined trajectories for synchronized observations. The spacecraft-to-spacecraft separations are variable between 20 m to 100m during observations to support various interferometer configurations in the planet-finding mode. The challenges involved with TPF autonomous operations, ranging from formation acquisition and formation maneuvering, to high precision formation flying during science observations are unprecedented for deep space missions. To meet these challenges, the Formation Sensor Testbed (FST) under the TPF technology program will develop and demonstrate the key technology of the formation acquisition sensor. Key performance targets for the acquisition sensor are an instantaneous 4π-steradian field of view and simultaneous range and bearing-angle measurements for multiple spacecraft with accuracy better than 50 cm and 1 degree, respectively. In this paper, we will describe the TPF FFI mission concept, the key formation flying challenges, the acquisition sensor design, the key design challenges, and the current plan to mitigate these design challenges.

TABLE OF CONTENTS

1. THE TPF MISSION

Terrestrial Planet Finder (TPF) is an important mission in the Navigator Program, the planet-finding part of NASA's Astronomical Search for Origins theme. TPF will support the Origins science goals by determining whether habitable or life-bearing planets are orbiting nearby stars. The mission will accomplish its goals by surveying as many as 150 solar type (F-, G-, and K-type) stars in the solar neighborhood, suppressing the radiation from the parent star and looking for the faint optical or infra-red reflection from planets in the "habitable zone." If bright planets are found, TPF will make low-resolution spectral observations, looking for evidence of habitability using markers like O_2, CO_2, and H_2O. Finally, TPF will make very sensitive low-resolution spectral observations of the most interesting planets using biomarkers such as O_2, O_3, and CH_4. The mission is scheduled to launch in 2015.

At present two architectures are competing for use on TPF: (1) a visible/near-infrared coronagraph and (2) a mid-IR nulling interferometer. The coronagraph has the advantages that: (1) we can achieve the required resolution with smaller optics at the shorter optical wavelengths, and (2) optical telescopes can operate at operate at ambient temperature (about 300 K), while a thermal IR telescope has to be cooled to about 40 K. On the other hand, the contrast between the star and planet is much stronger at visible (about 10^9) than at IR (10^6) wavelengths, with the consequence that the required suppression of stellar emission is much easier (but hardly easy) to achieve in the IR. Also, the individual apertures can be smaller in an interferometer (3–4 m) than in a coronagraph (6.5–8 m).

If the IR nulling interferometer is chosen, two further options have to be considered: (1) a structurally connected interferometer (SCI), in which the apertures are arranged along a single truss structure {Fig. 1?}, and (2) a formation flying interferometer (FFI) in which each collecting aperture and the beam-combining optics are on separate spacecraft that use thrusters and reaction wheels to maintain the required geometry {Fig. 2}. Again, each option has advantages. Obviously a rigid array is easier to control as it maneuvers and observes; and there is no risk that the optics will collide with one another or lose contact. But an array of spacecraft can achieve longer baselines (separations

between the collecting apertures) than are practical for a connected structure, and it is much more flexible in arranging the apertures appropriately for different observations. At the same time, the array requires constant management to maintain its integrity as it maneuvers and to maintain the required equality of optical paths (to a fraction of a micron) during interferometric observations.

Since 2002, two kinds of coronagraphs and the two interferometric options are undergoing evaluation and associated technology development. In 2006 an architecture will be chosen for the mission from these possibilities.

In the sections that follow, we focus on one of the technologies required for the FFI option: an "acquisition sensor" that maintains the integrity of the array throughout its lifetime and positions the spacecraft so that a more accurate relative sensor can assume control in preparation for interferometric observations.

2. Requirements on Formation Flying

The acquisition sensor provides observations from each spacecraft to a central processor that enable the processor to determine the relative locations of all the spacecraft in the array. Thus the sensor serves two functions: (1) It maintains the array in a known state, preventing both collisions between spacecraft and loss of spacecraft from the array. (2) It initializes the relative locations of the spacecraft for interferometry, so that the lines of sight of a sensor (or a succession of sensors) having a narrower field of view, but greater accuracy, can take over. In order to perform these functions, the acquisition sensor needs to satisfy the following requirements.

(1) The sensor must do its job well regardless of the eventual architecture of the array. At present various architectures are under consideration. Although the dual-chopping Bracewell architecture, with four similar collinear collectors and a combiner, is the current baseline, other architectures are under consideration; and the eventual choice may differ from the baseline both in the number of spacecraft and in their arrangement. We want a sensor that will work with any architecture.

(2) The sensor must be able to start from scratch. That is, the sensor on each spacecraft must be able to acquire the other spacecraft without any a priori information about their locations or velocities.

(3) Each spacecraft must be able to sense each other spacecraft that is not geometrically blocked. This feature is necessary for acquisition or recovery from any chaotic state.

(4) The sensor must be able to acquire some spacecraft while tracking others. This requirement is necessary for orderly acquisition, given that the procedures for acquisition and tracking are quite different.

(5) The sensor must be able to calibrate bearing angles without maneuvering the spacecraft. Bearing angles (elevation and azimuth, for example) are derived from the phase differences of a received signal at three or more receiving antennas. However, There is initially an *n*-cycle ambiguity in these differences. The ambiguities can be resolved by a number of schemes that involve translating or rotating the spacecraft. While these procedures may be tractable for two spacecraft, they are intolerable for a large array that could consist of seven or more elements.

(6) The sensor must be able to maintain the array if the sensor fails temporarily on one spacecraft. This requirement assures that thee will be no collisions or loss of spacecraft from the array after the sensor resets on one spacecraft, rendering it deaf and dumb for several minutes. A more serious outage might isolate a spacecraft for several days.

(7) The sensor must be compatible with the temperature distribution imposed by the IR telescopes: a warm side of the spacecraft, including most of the electronics, at something like 300 K and a cold side, including all the optics, at about 35 K.

Once these general requirements are met, the sensor must align all the spacecraft well enough so that a more accurate sensor with a smaller field of view can initialize itself. We therefore have the following performance requirements.

Requirement	Normal Operation	"Radar"
Operating envelope		
Inter-s/c range (m)	16–10,000	16–200
Inter-s/c bearing (sr)	4π	4π
Inter-s/c range rate (m/s)	2	2
Inter-s/c bearing rate (deg./s)	1	1
Range (m)	0.5	1.0
Range rate (m/s)	0.001	0.01
Bearing (degrees)	1	30
Bearing rate (arcmin/s)	1	–

Table 1. Performance Requirements for Acquisition Sensor

In Table 1, note that the operating range for the interferometer is 16-100 meters between centers. The envelope value allows for operation with reduced accuracy to 10 km for recovery from faults. For the radar mode, operation extends only to 200 meters because the signals are reflected.

The following section describes a sensor that meets these requirements.

3. Design Trades

Because of the constraints placed on the acquisition sensor by the spacecraft, and the performance requirements it must meet, it faces formidable design challenges. Below we

discuss some of these challenges and how they have been met.

Sensing Technology

The most fundamental choice to be made concerning the acquisition sensor is the sensing technology. Radio and optical are the obvious choices, and no other possibilities have been seriously considered. Considerations (3) and (7) above are crucial.

Optical sensors tend to have a relatively small field of view. Hence, to obtain global coverage one must either have a large number of them or extend their field of regard by scanning them. However, the number of individual sensors required for instantaneous coverage may be excessive, and scanning requires moving parts, which are to be avoided in the flight environment. Perhaps a stronger objection to scanning is that it requires motors, which generate heat. The problem with heat is that in order to get global coverage, some of the sensors must be placed on the cold side of the spacecraft. Since the spacecraft are passively cooled to 35 K, heat sources must be strictly limited at the milliwatt level.

Another problem that militates against optical sensors is the sun. When the sensing direction approaches the sun, as it may, it is hard to prevent sunlight from saturating or otherwise confusing the sensor. We might try to overcome this problem by using a spectrally narrow (laser) signal and a correspondingly narrow filter on the input, but there is difficulty in making the filter narrow enough to discriminate effectively in favor of the signal and at the same time wide enough to allow for the width of the signal and the variability of the signal and filter.

RF sensors have problems of their own, but they appear more manageable. Multiple antennas are needed to achieve complete directional coverage, but they can have a wide field of view, and there are no moving parts. Nevertheless, heat transfer to the cold side of the spacecraft remains a problem, because transmission lines must connect the cold-side antennas with the warm electronics. Heat is conducted along these lines, and for the transmitters, signal power is dissipated as well. On balance, an RF sensor is preferable.

RF Frequency

Having chosen an RF sensor, we have to pick the frequency at which that sensor will operate. The discriminators are system temperature, multipath, spacecraft accommodation, and allocation. We can't simply select a convenient frequency based on the needs of the mission: we have to fit into an allocation of the National Telecommunications and Information Administration (NTIA) and the International Telecommunications Union (ITU). Table 2 shows the bands that are available for spacecraft-to-spacecraft communication between 1 and 100 GHz [1].

BAND	FREQUENCY
S	2025–2110 MHz
	2200–2290 MHz
Ku	13.75–14.30 GHz
	14.50–15.35 GHz
Ka	22.55–23.55 GHz
	25.50–27.00 GHz
	32.30–33.40 GHz
W	59–64 GHz
	65–71 GHz

Table 2. Frequency Allocations

Among these frequencies, phase multipath, proportional to wavelength, is smaller at the higher frequencies. However, this factor is not crucial, because the requirement on bearing (whose accuracy depends mostly on the phase observable) is fairly relaxed. The lowest frequencies (at S band) have the great advantage that we can use coax rather than waveguide for the RF transmission lines. Furthermore, system temperatures are smaller at the lower frequencies. As a bonus, S-band hardware is generally less expensive than it is at the higher frequencies. On the whole, S band meets the requirements most easily and is our choice.

Signal Structure

Recall that the acquisition sensor has 4 functions:
(1) It acquires the signals transmitted by other spacecraft.
(2) Having acquired the signals, it makes measurements that allow the determination of the ranges to the other spacecraft.
(3) It also makes measurements that allow the determination of the directions of the other spacecraft. (These directions are in a local reference frame that moves with the receiving spacecraft, and they might be expressed as azimuth and elevation, for example.)
(4) If the sensor on one of the spacecraft fails temporarily (because of a power interruption, for instance), the other spacecraft maintain the array indefinitely, preventing their disabled comrade from drifting out of contact or colliding with one of the others.

Designing a signal structure that fulfills these requirements expediently requires some subtlety, and we draw heavily on our experience designing GPS receivers. Range is determined in the first instance by a pseudo-random (PR) ranging code modulated onto a carrier, and bearing angles are calculated from the phase differences of carriers arriving at different antennas, as shown in Figure 3. For simplicity, the figure shows only one bearing angle and two antennas; to determine both angles, the signal must be received at three antennas.

A complication of the bearing-angle determination is that there is an integer-cycle ambiguity in measuring the phase difference between signals received at two antennas, and generally the range determinations are not good enough to resolve the ambiguity. We can resolve the ambiguity in

several ways by maneuvering the spacecraft, using either rotation or translation. However, since the maneuvers consume precious time during acquisition, have to be repeated whenever the receivers "lose lock" on a signal, and involve several spacecraft, this solution was rejected as impractical. It would be better to use a signal structure that resolves the ambiguity internally, precluding the need for maneuvers.

Such a signal structure has been devised [2,3], and as explained below, it also speeds acquisition. As shown in Figure 4, this signal is a generalization of binary offset carrier (BOC) that we informally call "ultra-BOC." It consists of a central carrier modulated by a pseudo-random noise (PRN) code at 10 Mchips/s, two inner tones modulated slowly with data at about 100 bits/s, and two outer tones that are unmodulated. (The central component may also be modulated with data at perhaps 10 kbit/s, but that modulation does not bear on the current discussion.)

With this signal, acquisition starts with an outer tone, which is easy to find because it requires a search over frequency but not time. Once this tone is found, we know from the frequency which transmitter sent it and can do a relatively short search for the inner tone, whose modulation contains some fixed bits and a time code, perhaps at intervals of a second. Knowing the time, we then do another short search over delay to acquire the rapid modulation on the central carrier.

Generation of the observables proceeds in the opposite sense, working from the central component outward. In the first step, we start from the delay given by the ranging code. Then we form a "synthesized delay" by using the closely spaced tones on one side (either side) of the center frequency. That is, we compute

$$\Delta\tau = (\phi_1 - \phi_2)/(\nu_1 - \nu_2), \qquad (1)$$

where the ϕ's are the observed phases at the two frequencies and the ν's are the frequencies themselves. Because the integral cycles of phase are unknown for each measurement, there is an n-cycle ambiguity in the phase difference. We resolve this ambiguity using the known delay from the ranging code. For the procedure to work, the error in the ranging-code delay must be much less than the error made by offsetting the phase difference by a half cycle. Furthermore, the instrumental components of the phases must have been calibrated to a small fraction of a cycle. Hence the procedure is more likely to succeed for the differential phases (between receiving antennas) used to compute bearing angles than for the undifferenced phases that could be used to compute ranges.

In the second step of the ultra-BOC procedure, we continue in the same way, forming a second synthesized delay from the two outer tones. This step helps because the error in the delay determination is proportional to $1/(\nu_1 - \nu_2)$, which obviously decreases as the frequency difference increases. The same caveats discussed above apply.

In the third step of the ultra-BOC procedure, we expect to resolve the phase ambiguity at the carrier frequency itself. In any case, we have succeeded in removing the integer-cycle phase ambiguity from the differential phase measurements using the signals alone: no spacecraft maneuvers are necessary.

Before leaving the subject of ultra-BOC, we need to determine what are the optimum spacings of the various components. Without going into the details of the calculations, we can say that Eq. 1, along with the assumptions that (1) the error on the output delay at each step is much smaller than the error on the input delay, and (2) the error on the input delay at each step is less than 1/6 of the delay ambiguity at the output of that step (so that the probability of an error at each step is approximately 0.0027), leads to

$$\Delta\nu_1 \le \frac{c}{6\sqrt{2}\sigma_\rho}, \qquad (2)$$

$$\frac{\Delta\nu_2}{\Delta\nu_1} \le \frac{1}{6\sqrt{4}\sigma_\phi}, \qquad (3)$$

and

$$\frac{\nu_{rf}}{\Delta\nu_2} \le \frac{1}{6\sqrt{4}\sigma_\phi}, \qquad (4)$$

where σ_ρ is the system-noise error on range,
λ_{ch} is the chip length of the PRN code, here equal to c/(10 MHz) = 30 m,
$\Delta\nu_1$ is the frequency difference of the narrow separation (Hz),
$\Delta\nu_2$ is the frequency difference of the wide separation (Hz), and
σ_ϕ is the uncertainty of an undifferenced phase measurement (cycles).

Assuming that σ_ρ = 0.5 m and σ_ϕ = 0.01 cycle, we have tentatively chosen. $\Delta\nu_1$ = 40 MHz and $\Delta\nu_2$ = 300 MHz to go along with ν_{rf} = 2200 MHz.

Antenna Configuration

Getting true instantaneous 4π-steradian coverage requires many antennas. If each antenna's beam extends to 70° off boresight, then it can see almost a third of the sky. Allowing for overlap of the beams (unavoidable if we are to attain complete coverage), it will take four transmitting antennas to cover the entire sphere. These antennas are most simply pointed in the directions of the vertices of a regular tetrahedron, as shown in Figure 5. In that case, the beamwidth required for complete coverage is $\cos^{-1}(1/3)$ = 70.53°.

Since we need three receiving antennas to be visible from any direction, in order to sense the two bearing angles of the transmitter, we expect to need about three times as many receiving antennas as transmitting antennas, or twelve.

These antennas can point toward the vertices of a regular icosahedron, as shown in Figure 6. The beam angle needed to have three antennas looking in every direction is then $\cos^{-1}\left(1/\sqrt{5}\right) = 63.43°$, which is in fact the angular separation of neighboring antennas.

In all, therefore, this scheme involves 16 antennas, which might be placed as shown in Figure 7. It should be remembered that the issues of (a) the directions of the antenna beams and (b) the placement of the antennas, are distinct but related. One would expect the beam to point outward from the spacecraft at the point of attachment, but the beam size and the spacecraft structure in the neighborhood of the antenna may allow some latitude in direction at a given point.

Another issue, at least for receiving, is the distribution of antennas over the spacecraft. In principle, we might gain some advantage by clustering receiving antennas together at convenient points. However, the arithmetic of the bearing-angle measurements makes this clustering difficult or impossible. Imagine that we are on a transmitting spacecraft, looking at the projection onto the plane perpendicular to the line of sight of the triangle whose vertices are the three receiving antennas, as shown in Figure 8. The uncertainty of a bearing angle of the transmitter, as seen from the receiving spacecraft, is inversely proportional to the projection of the triangle onto the associated coordinate direction. Thus, if the triangle is thin, the bearing-angle determination in the thin direction is relatively bad. Consequently neighboring antennas need to be well separated and uniformly distributed in all directions if the bearing angles are to be well determined.

A final problem for antenna distribution is the presence of the thermal shield, because it effectively partitions the observable directions into two distinct hemispheres, those above and those below the shield. Since the shield is by definition thermally opaque, it tends to be opaque to RF energy as well: a transmitter or receiver on one side of the shield can't penetrate to the other side. This circumstance complicates sensing near the plane of the shield, which is crucial, since the shields of all the spacecraft are in the same plane during interferometry. The solution adopted in the placement of Figure 7 is to place antennas near the edge of the shield, where they can peek around it.

The current plan is to use a total of 16 antennas on each spacecraft. If this number is unacceptably large, at least two means of reduction are available, alone or in combination:
(1) *Use wider beams.* For, example, if the beams extended to 90° off axis, we could in principle get the required coverage with two transmitting antennas and six receiving antennas per spacecraft. However, the on-axis gain would be lower, multipath would be stronger, and the placement of the antennas would be limited to locations with a hemispherical field of view.
(2) *Relax the requirements.* For instance, we might decide that we need less accuracy in directions not needed for handoff to another relative sensor. In that case we could concentrate our antennas in the handoff directions and reduce the number in directions used only for acquisition. However, we might have to give up considerable performance in order to get a worthwhile reduction in the number of antennas.

At present, all options are open with respect to placement of the antennas, and accommodation with the spacecraft will evolve as the spacecraft itself develops.

Interference between Signals

In any particular receiving channel, we may have the wanted signal from a remote spacecraft, unwanted (because they contribute to receiver "noise") signals from other remote spacecraft (or possibly from another transmitter on the same remote spacecraft), and unwanted signals from transmitters on the local spacecraft. The local signals, in particular, may saturate the front end of the receiver and cause severe loss of SNR in the wanted signal. In addition, we need to be able to identify the transmitted signals with their spacecraft and discriminate among them in signal processing.

We can deal with these problem in several ways. One way is code-division multiple access (CDMA), which we intend to use to distinguish among the BPSK-modulated central components of the ultra-BOC signal structure: Like GPS signals, each transmitter has its own code that enables the receivers to distinguish and identify them. Another way is frequency-division multiple access (FDMA): We expect to space the ultra-BOC tones a little differently on all the transmitters, so that the tones (and data sidebands) won't interfere with one another.

Still another way is time-division duplexing to reduce interference, especially from the transmitters on the same spacecraft as a receiver. This scheme involves transmitting and receiving alternately, so that the transmitted signal can't interfere with reception.

One way to do this is to have the spacecraft take turns transmitting and receive the rest of the time, as shown in Figure 9a. This approach minimizes transmissions and prevents interference between spacecraft completely. On the other hand, it requires synchronization among the spacecraft and would be awkward to implement for all possible situations in a multiple-spacecraft array involving acquisition, non-functioning spacecraft, and so on.

An easier procedure to implement is for each spacecraft to take turns transmitting and receiving without consideration of what the other spacecraft are doing. The most straightforward approach is to follow a fixed pattern, for example transmitting for a certain interval and then receiving for an equal interval and repeating the pattern, as shown in Figure 9b. In this case the spacecraft should use different intervals to assure that over a period of many intervals, each spacecraft receives each of the others equally. A typical interval for transmission or reception might be 100 μs. Of course, this approach has the disadvantage that the remote spacecraft will interfere with one another's signals, but it does avoid interference from the local spacecraft.

A more exotic approach is to switch the transmitters on and off at equal intervals according to a pseudo-random code that is different for each spacecraft [4], as in Figure 9c. The reason behind this apparently gratuitous complexity is that for any two-way travel time longer than a chip of the code, a transmitted signal can bounce off a remote spacecraft and have a 50% chance of arriving back at the local spacecraft a time when the transmitter is off and the receiver is on. Thus, the signal can be used for radar detection of a spacecraft whose coarse sensor is temporarily down. Obviously the chipping rate has to be high for this technique to work for closely spaced spacecraft. If we insist that half the return take place while the receiver is on, then for a minimum distance of 15 m between two spacecraft, the chipping rate has to be at least 10 MHz.

At present, the baseline transceiver design includes CDMA and FDMA as described above. The form of time duplexing to be used is still under consideration.

Heat Transfer

Heat transfer from the warm side (~300 K) of the spacecraft to the cold side (~40 K) containing the infrared optics must be absolutely minimized. Quantitative limits are now being developed, but it's clear that milliwatts are significant, since the ability of the cold side to lose heat passively by radiation is limited. The acquisition sensor is implicated in this problem because of the coax cables connecting the transceiver, on the hot side, with antennas on the cold side. These cables can heat the cold side in two ways: by conduction through the metal conductors and by dissipation of power being carried from the transmitters.

To get an idea of the magnitude of the problem, consider 50 Ω 32081 coaxial cable. Analysis [5] shows that the heat loss to be expected from one of these cables, of the length necessary to connect the transceiver to an antenna on the cold side of the spacecraft (~5 m), through the temperature difference indicated above, is on the order of 30 mW. Furthermore, the dissipation of energy carried along the cable at S band is about 1 dB/m, so we can expect to lose about 68% of the original power along the way. If 10 mW reaches the antenna, then we lose about 22 mW along the way, and some of that will heat the cold side.

There are several ways in which this heat input to the cold side can be reduced. One is to minimize the number of antennas there, particularly transmitters. We can get by with a single transmitting antenna on the cold side if the others are allowed to peek upward from the warm side around the edge of the heat shield. Another way is to turn off transmissions to antennas on the cold side when they are not being used. For example, we could certainly arrange for warm-side transmitters to do the sensor's work while the array is in the normal observing configuration for interferometry. A third way would be to make the transmission lines from materials that have high electrical conductivity but low thermal conductivity; unfortunately, according to the Wiedemann-Franz Law [6] the two are proportional for metals (both alloys and pure metals), so that avenue appears unrewarding. However, since the high-conductivity region of the cable needs to be only a few skin depths thick (and the skin depth for copper at S band is only about 1.4 μm), we could, for example, use silver- or copper-plated stainless steel inner and outer conductors to get good electrical conduction while obstructing the flow of heat. [7]

The true magnitude of the problem is still unknown, since thermal models are only now being developed, and coarse-sensor transmission lines are only one of the sources of heat leakage. Furthermore, the radiating area on the cold side can be made large, so that if the heat conduction and emissivity are made high enough, a leakage rate of several watts can be accommodated at a temperature of 40 K. In view of practical limitions, however, the spacecraft may not be able to support a leakage rate of more than a few tenths of a watt.

4. THE SENSOR

Guided by the issues discussed in the preceding section, and others, we have designed a sensor, shown in Figure 10, that fulfills the requirements for an acquisition sensor for TPF. The generation of the transmitted signals begins at the upper left in the baseband processor. There is one transmission channel for each transmitting antenna, or four in all. In each channel, the low- and high-rate data of the ultra-BOC signal are combined with codes at the rates specified by frequency f_{tx} and a real-time clock (RTC). These signals then go to the RF section, where they are combined (mixed or added, as shown at the lower right) first with the offset of the inner ultra-BOC tone from the center frequency (see Figure 4), f_{b1}, then with the offset of the outer tone, f_{b2}, and finally with the carrier, f_c. The power level is set either to P_1 or P_2, depending on the proximity of the remote spacecraft. A very small part of the transmitted signal is routed to appropriate receivers on the same spacecraft to be used as a calibration signal. The rest passes through a switch (SW) that turns the signal off and on to prevent interference with reception.

In the receivers, after being picked up by an antenna, the remote signals pass through a switch that allows reception only when the local transmitters are off. Then the local calibration signals are injected, as needed, and the composite signal goes through a low-noise amplifier (LNA), bandpass filter (BPF), another amplifier, and finally an A/D converter before going to the baseband processor. In the baseband processor the signal is downconverted and correlated with the appropriate PN code to determine the range from the central ultra-BOC signal. This processing resembles the GPS paradigm, with early, prompt, and late integrations to find the peak of the correlation. Each of the significant components of the ultra-BOC signal is processed independently.

The tracking processor controls the entire process, accepting input from the spacecraft computer, extracting phase and delay observables, recovering the data bits (both fast, on the central component, and slow, on the inner ultra-BOC

tones), averaging and calibrating the observables, assigning time tags to them, and finally sending the calibrated observables to the spacecraft at one-second intervals. This processor also controls the power output of each of the transmitters and switches the transmitters and receivers off and on according to one of the schemes discussed above.

Central to the whole process are a frequency standard and synthesizers that provide coherent signals to the various parts of the sensor for generating and demodulating the components of the ultra-BOC signal, controlling sampling, and keeping time.

5. TESTBEDS

The acquisition sensor is complicated and contains many pieces of unproven technology. The TPF Project can ask, for example: Can the receiving and transmitting antennas be accommodated on the spacecraft? Can the sensor really attain 4π-steradian coverage? Can multipath be managed adequately? Can the data be calibrated well enough so that ultra-BOC will work as intended? Can we track a combination of close and distant spacecraft? Can we hand off gracefully from one antenna to another as the bearing angles change? Can the computational machinery keep up with all the model calculations, correlations, calibrations, I/O, and other functions required for a complex signal? All these technologies must be shown to work on the ground before they can fly. In fact, they must be proven before the TPF Project selects a mission architecture in 2006.

To validate the various new technologies, two ground testbeds have been devised. The first is an indoor testbed, shown schematically in Figure 11. Here three "spacecraft" will be connected by cables with attenuators adjusted to simulate space loss. This testbed will demonstrate:

1. That we can generate and interpret the ultra-BOC signal with the needed accuracy,
2 That we have the dynamic range to cope with a mixture of close and distant spacecraft,
3. That internal calibration works well enough to make ultra-BOC feasible,
4. The operation of the software being written to manage the sensor, and its interaction with the hardware, and
5. The ability of the software to keep up with the required computations.

However, the full functionality of the sensor can be demonstrated only in a spacecraft-like environment. For this purpose we are designing a second outdoor testbed, shown conceptually in Figure 12. It will be implemented after the indoor testbed has done most of its work and will build on the validation achieved there. In the outdoor testbed the RF signals will be broadcast through the air between actual antennas mounted on three realistic models of the spacecraft that can be translated and rotated. The outdoor testbed will demonstrate:

1. 2π-steradian coverage with two transmitting antennas and six receiving antennas on one modeled spacecraft, including handoff from one antenna to another as the bearing angles of the remote spacecraft change,
2. Operation of ultra-BOC in a realistic environment, giving bearing angles without calibration maneuvers,
3. Satisfaction of the performance requirements, confirmed by truth sensors, between 16 and 1000 m range,
4. Operation of the radar mode, with the sensor disabled on one spacecraft,
5. Management of multipath adequate to meet the performance requirements, and
6. Ability of the sensor to track a distant spacecraft in the presence of one nearby.

Together, these two testbeds will provide the means to advance the technology level of the sensor to flight readiness. They will show that the sensor can do its part to make formation-flying interferometry an attractive option for the TPF Mission.

6. SUMMARY

Formation-flying interferometry is a proposed architecture for TPF, a mission to detect Earth-like planets orbiting nearby stars. However, such an architecture requires a reliable "acquisition sensor" that can maintain the integrity of an array of at least five spacecraft and position them for handoff to another sensor for more accurate control. According to current requirements, the acquisition sensor would need to have a 4π-steradian field of view and provide relative positioning between spacecraft with an uncertainty of 50 cm in range and 1° in the bearing angles, at separations of 16 to 10,000 m.

Such a sensor does not exist and faces formidable technical challenges. First, the technology must meet the requirements while co-existing with the spacecraft and interferometer. At the same time, the signal structure must facilitate acquisition of the signal, expedite calibration, meet the performance requirements, and tolerate failures. Finally, the sensor must operate reliably for at least five years and scale gracefully from five to seven or more spacecraft.

We have designed a sensor to meet these requirements. To develop the new technology we are building two testbeds, one indoors and one outdoors, that will validate the various elements singly and in combination. The indoor testbed will provide maximum control for debugging, and the outdoor testbed will provide maximum fidelity to the actual operating environment for a subset of the flight sensor.

REFERENCES

[1] National Telecommunications and Information Administration, *Manual of Regulations & Procedures for Federal Radio Frequency Management*, U.S. Government Printing Office, Washington, D.C., May, 2003.

[2] NTR

[3] George Purcell, *Error Calculations for Use of BOC 2 Signal Structure to Resolve Integer-Cycle Ambiguities in the*

Coarse Sensor's Single-Differenced Phase Observable, JPL Internal Memorandum, December 30, 2002.

[4] Jeff Tien NTR on random switching

[5] Ray Garcia's analysis

[6] H.M. Rosenberg, "The Behavior of Materials at Low Temperatures," *Advanced Cryogenics*, ed. C.A. Bailey, New York, Plenum Press, 1971, pp. 77–101.

[7] Sander Weinreb, *Cryogenic Performance of Microwave Terminations, Attenuators, Absorbers, and Coaxial Cable*, National Radio Astronomy Observatory Electronics Division Internal Report 223, Charlottesville, Virginia, January, 1982.

BIOGRAPHY

Jeffrey Srinivasan received an A.B. degree in Engineering and Applied Sciences from Harvard College in 1983 and a M.S. degree in Electrical Engineering from the University of Southern California in 1988. Since 1983, he has worked at NASA's Jet Propulsion Laboratory in Pasadena, California. He has focused on developing high accuracy, flexible GPS receivers, first for terrestrial applications and, later, for space flight. Currently the Technical Supervisor of the Advanced Radio Metric Instruments Development Group, Mr. Srinivasan is working to extend the application of Science-grade GPS instruments to precision formation flying missions like TPF, further advancing JPL and NASA's science data collection goals.

George Purcell has been a member of the Technical Staff at the Jet Propulsion Laboratory since 1975. His research interests and experience include radio interferometry and its geodetic applications, GPS applications, experimental design, and data analysis. Since 1998 he has been working on the development of formation flying technology for StarLight and TPF.

Jeffrey Tien received his M.S. degree in Electrical Engineering from USC in 1993. He joined the GPS systems group at JPL in 1989 where he worked on hardware design of flight GPS receivers for various space missions. He has served as the Instrument Lead Engineer for the Autonomous Formation Flying sensor on the StarLight Mission for the last two years. His research interest includes high speed signal processing and formation flying sensor technology development

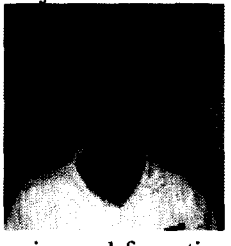

Dr. Larry E. Young has developed radiometric technology at Caltech's Jet Propulsion Laboratory since 1978. Specific areas of his group's research include digital GPS receivers, multipath mitigation, sub-nanosecond clock synchronization, satellite-based science applications of GPS receivers, and sub-cm formation flying. He has served on several committees defining future navigation systems.

TABLES

1. Performance Requirements
2. Frequency Allocations

FIGURES (those shown in red do not yet exist)

1. Structurally Connected Interferometer
2. Formation-Flying Interferometer
3. Bearing Angle Determination
4. Ultra-BOC Signal Structure
5. Geometry of Transmitting Directions
6. Geometry of Receiving Directions
7. Locations of Antennas on Spacecraft
8. Receiving Antennas As Seen from Transmitter

9a. Synchronous Transmission and Reception

9b. Asynchronous Transmission and Reception

9c. Pseudo-Random Transmission and Reception

10. Block Diagram of Recceiver
11. Indoor Testbed (Schematic)
12. Outdoor Testbed (Conceptual)

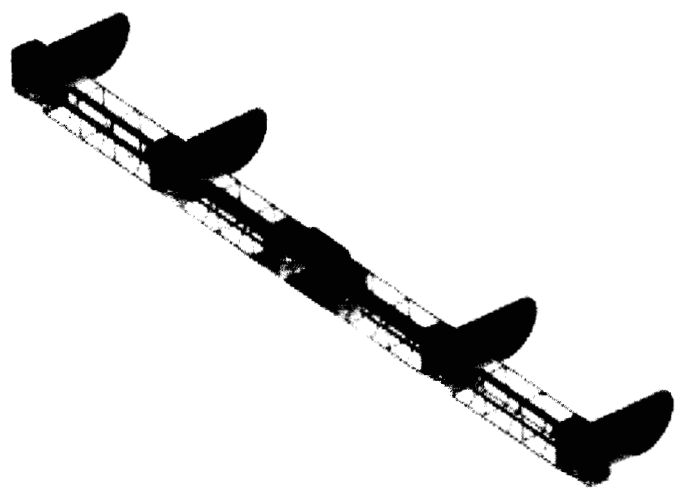

Figure 1. Structurally Connected Interferometer

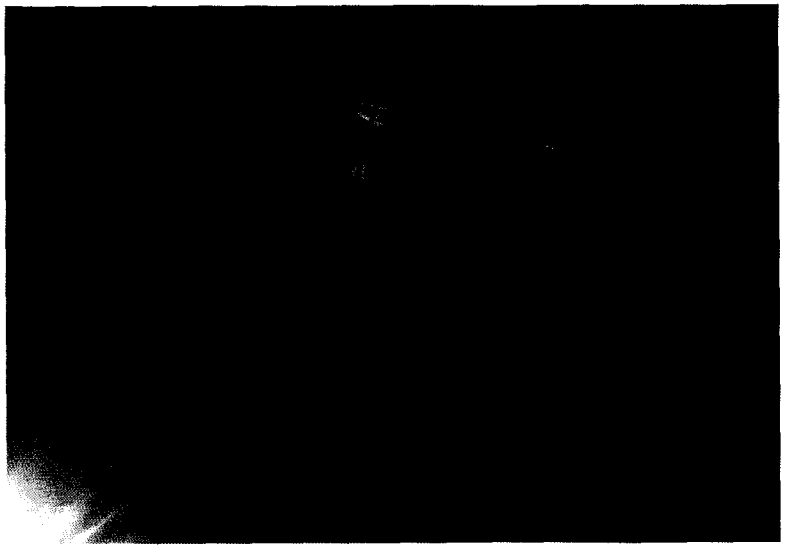

Figure 2. Formation-Flying Interferometer

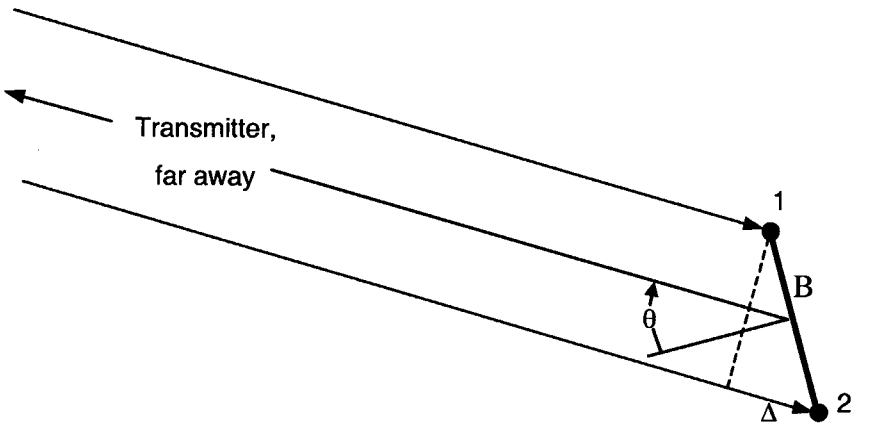

Baseline = B

Excess range at antenna 2 = Δ

Bearing angle $\theta = \sin^{-1}(\Delta/B)$

Figure 3. Bearing Angle of Transmitter

Figure 4. Ultra-BOC Signal Structure

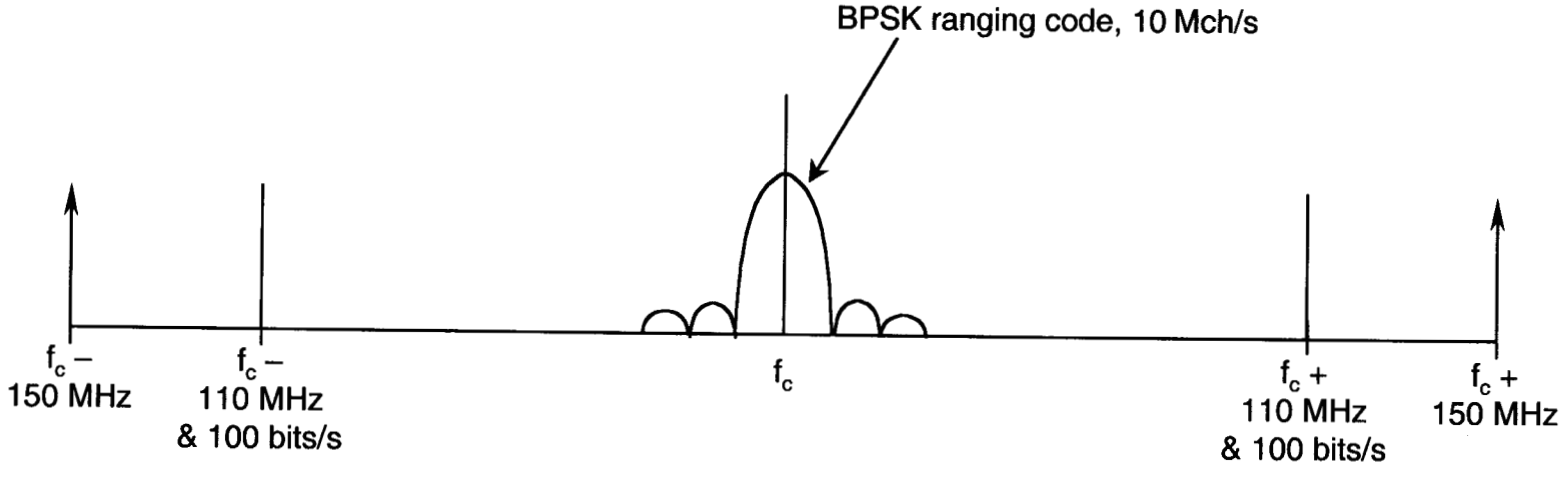

Figure 5. Geometry of Transmitting Directions

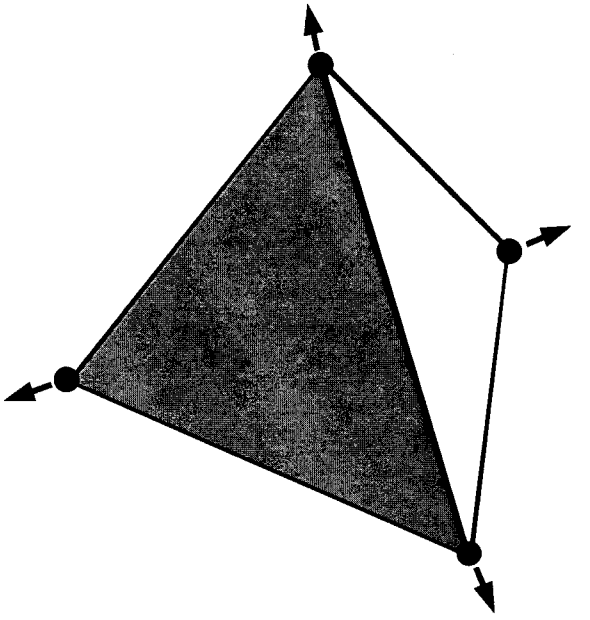

Figure 6. Geometry of Receiving Directions

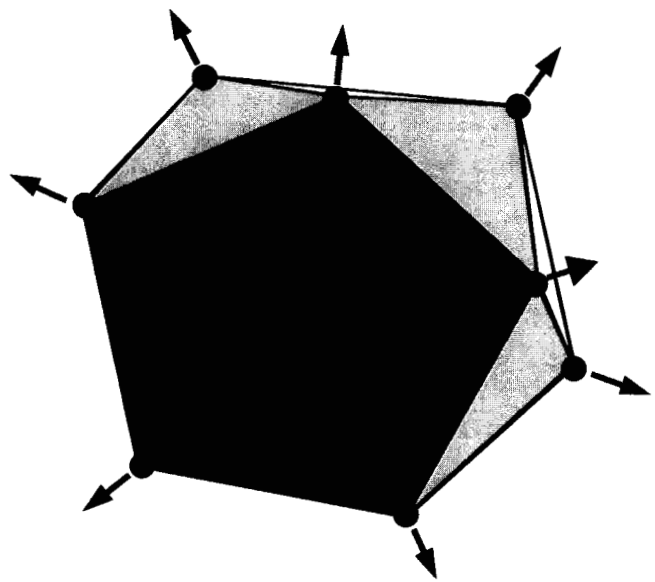

Figure 7. Possible Locations of Antennas on Spacecraft

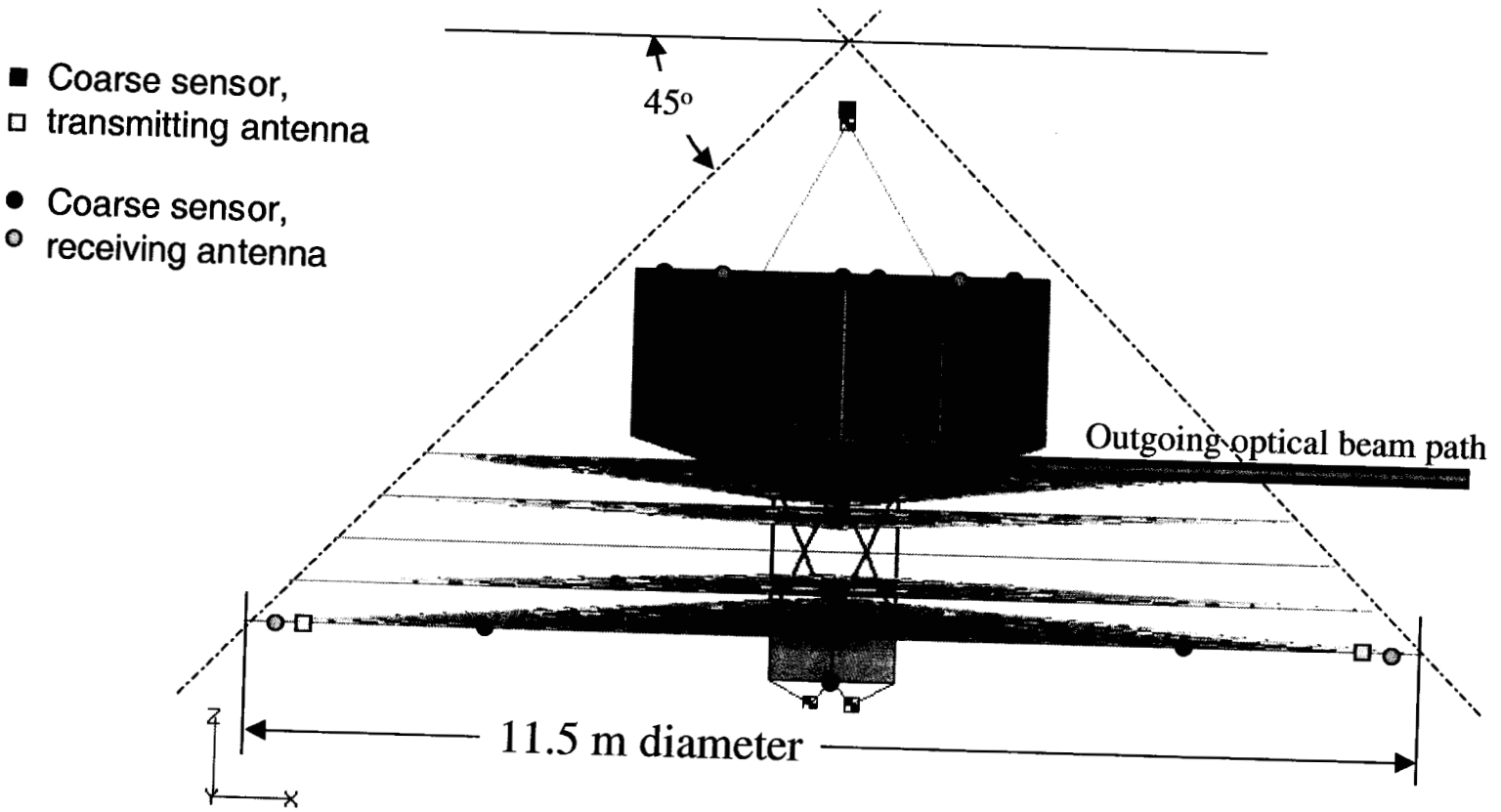

Figure 8. Receiving Antennas As Seen from Transmitter (Schematic)

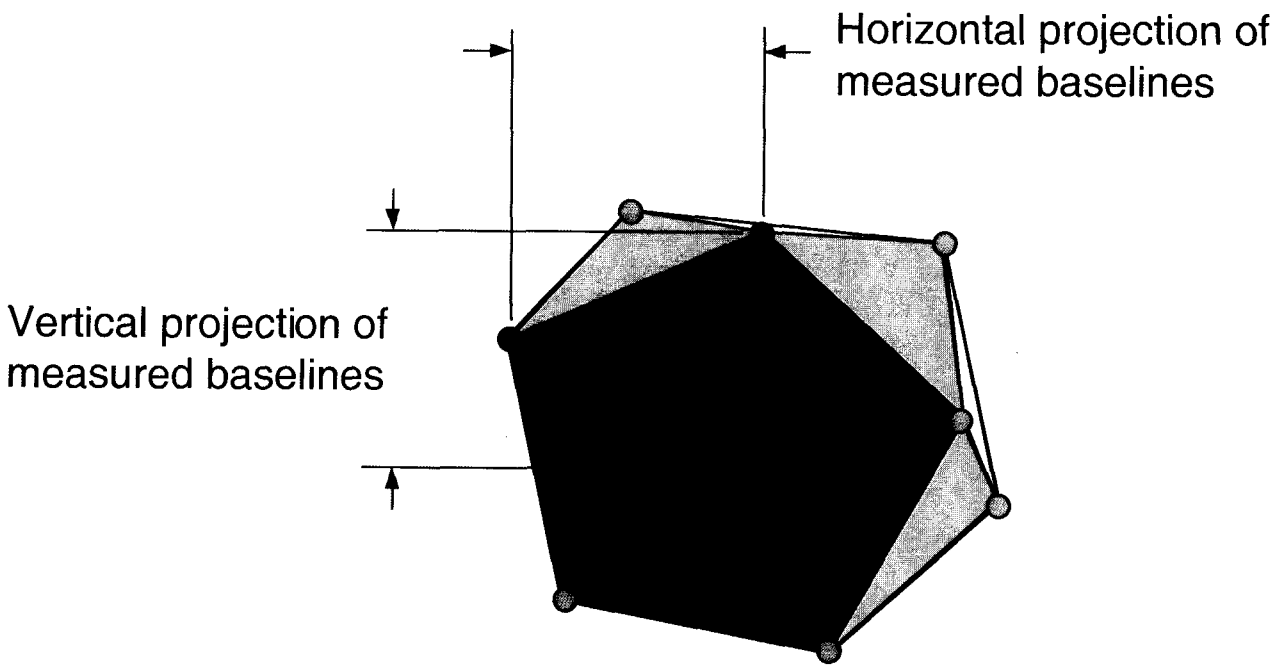

Figure 9. Coordination of Transmission and Reception To Reduce Interference

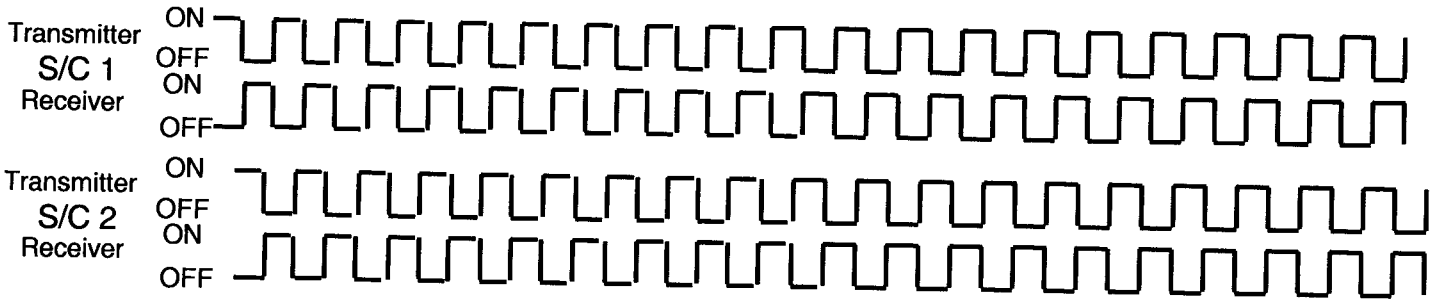

Figure 9a. Asynchronous Transmission and Reception

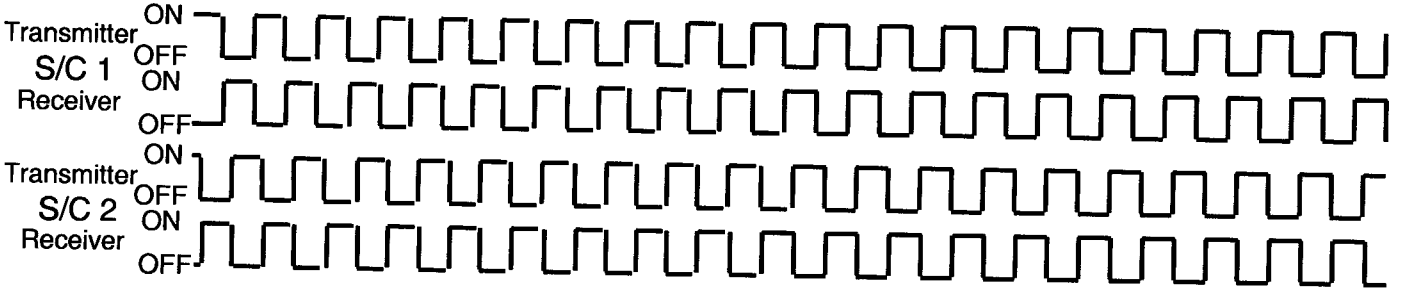

Figure 9b. Synchronous Transmission and Reception

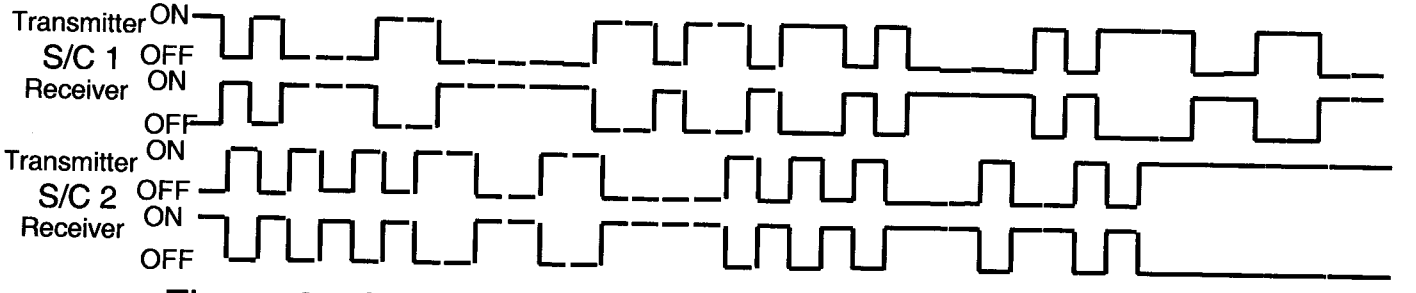

Figure 9c. Pseudo-Random Transmission and Reception

Figure 10. Acquisition Sensor Functional Block Diagram

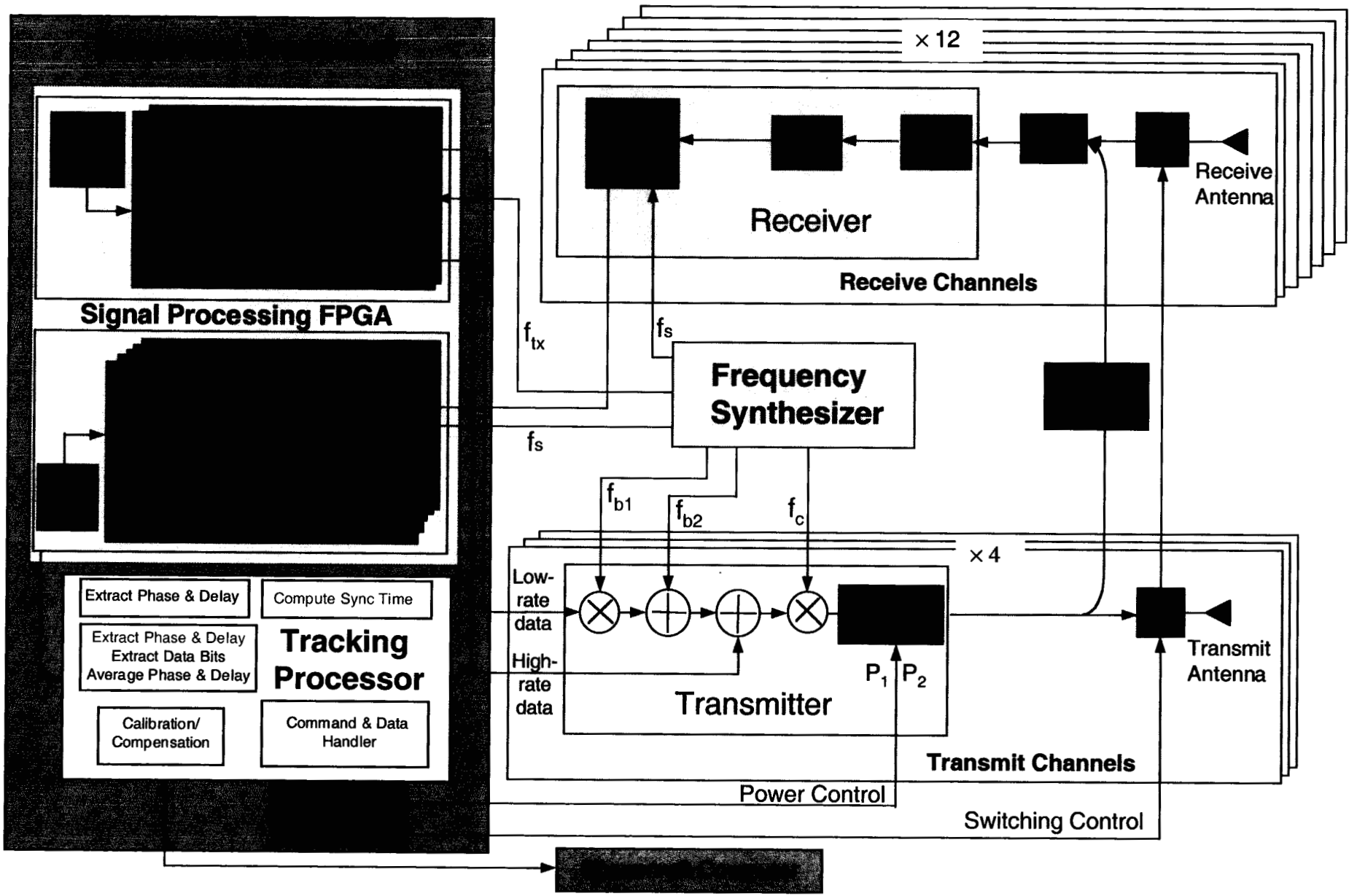

Figure 11. Indoor Testbed (Schematic)

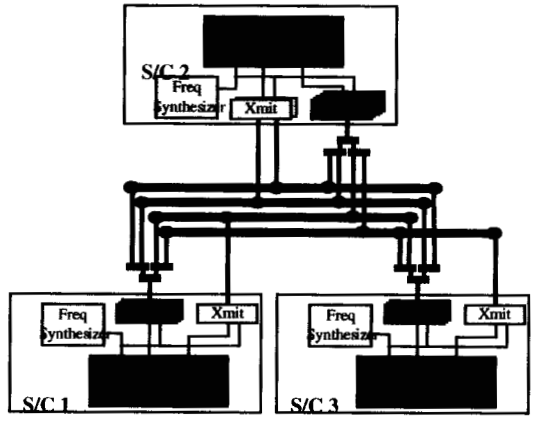

Indoor Functionality Testbed

Figure 11 alt. Indoor Testbed (Schematic)

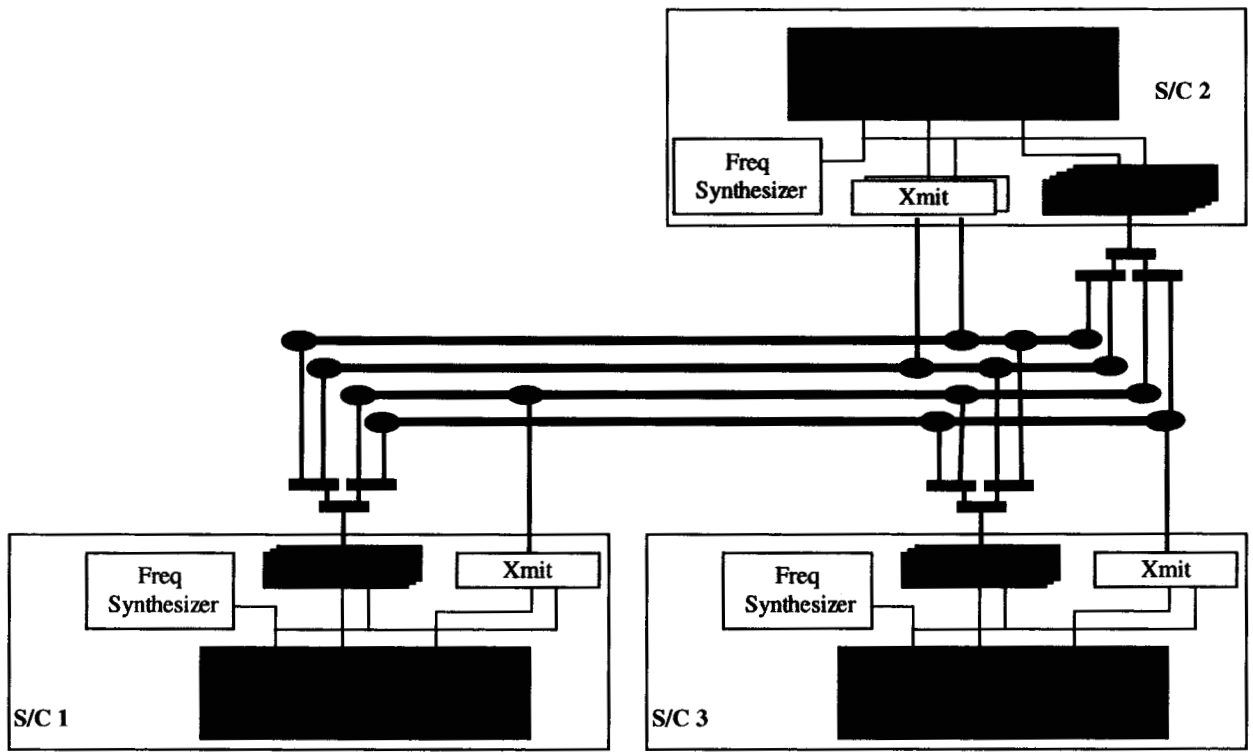

Figure 12. Outdoor Testbed (Concept)

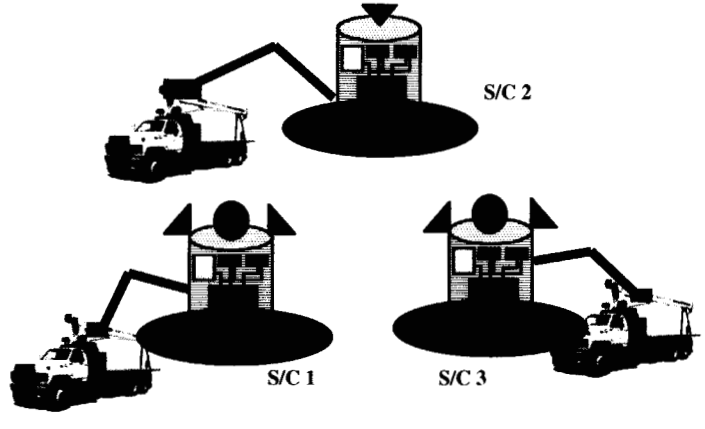
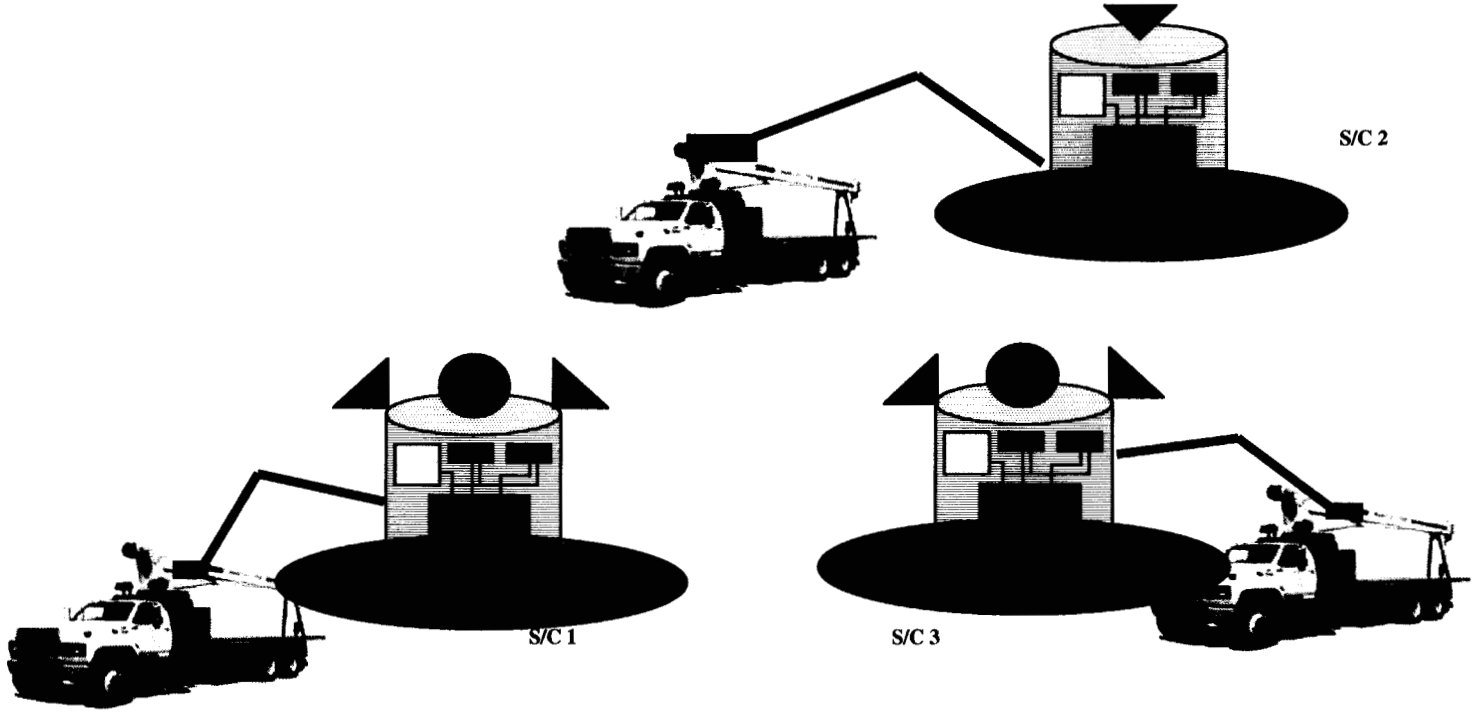
Figure 12 alt. Outdoor Testbed (Concept)